



OPEN ACCESS

EDITED BY
Rui Yong,
Ningbo University, China

REVIEWED BY
Pengpeng Ni,
Sun Yat-sen University, China
Mahmood Ahmad,
University of Engineering and Technology,
Pakistan
Menglim Hoy,
Suranaree University of Technology, Thailand

*CORRESPONDENCE
Weifeng Zheng,
✉ teresastores85@gmail.com

†These authors have contributed equally to
this work

RECEIVED 07 March 2024
ACCEPTED 08 April 2024
PUBLISHED 24 April 2024

CITATION
Zhou M, Zheng W, Han Y and Tang C (2024),
Analysis of fly ash-treated SDCM pile behavior
through laboratory model tests.
Front. Earth Sci. 12:1397339.
doi: 10.3389/feart.2024.1397339

COPYRIGHT
© 2024 Zhou, Zheng, Han and Tang. This is an
open-access article distributed under the
terms of the [Creative Commons Attribution
License \(CC BY\)](https://creativecommons.org/licenses/by/4.0/). The use, distribution or
reproduction in other forums is permitted,
provided the original author(s) and the
copyright owner(s) are credited and that the
original publication in this journal is cited, in
accordance with accepted academic practice.
No use, distribution or reproduction is
permitted which does not comply with
these terms.

Analysis of fly ash-treated SDCM pile behavior through laboratory model tests

Min Zhou^{1,2,3†}, Weifeng Zheng^{4*†}, Yunshan Han^{1,3} and
Changyi Tang^{5,6}

¹School of Environment and Safety Engineering, North University of China, Taiyuan, China, ²Shanxi Construction Investment Group Co., Ltd., Postdoctoral Research Workstation, Taiyuan, China, ³Shanxi Graduate Education Innovation Center of Underground Space Engineering, Taiyuan, China, ⁴Institute of Foundation Engineering, China Academy of Building Research, Beijing, China, ⁵Zhuhai Institute of Urban Planning & Design, Zhuhai, China, ⁶School of Civil Engineering, Southwest Jiaotong University, Chengdu, China

Fly ash, an industrial byproduct, has resulted in significant environmental pollution and poses a threat to human health due to its low recovery and utilization rate. Stiffened deep cement mixing (SDCM) piles, leveraging both the high lateral friction resistance of cement mixing pile socket and the high strength of concrete core pile, are widely employed in practice of soft ground improvement. However, to avoid damage to cement mixing pile socket, a higher amount of cement is often required, leading to not only elevated project costs but also conflicting with low-carbon environmental objectives. In tackling this concern, the introduction of fly ash as a partial substitute for cement in cement mixing pile socket offers a solution. This study delves into the vertical bearing mechanism of fly ash-treated SDCM piles through laboratory model tests. Results reveal that as the curing duration extends, the hydration rates of fly ash decrease relative to cement, being demonstrated by larger settlements at the top of fly ash-treated SDCM pile compared to that of standard SDCM pile. It is also found that elevated levels of hydration in cement mixing pile socket results in a heightened stiffness and an enhanced pile end resistance.

KEYWORDS

stiffened deep cement mixing (SDCM) pile, fly ash, model test, core pile, pile end resistance

Introduction

Fly ash is a fine particulate matter obtained from flue gas of coal powder combustion in boilers, typically comprising spherical particles with smooth surfaces. It constitutes the primary solid waste discharged by coal-fired power plants. The major constituents of fly ash encompass SiO_2 , Al_2O_3 , Fe_2O_3 , and CaO , etc., with the particle sizes ranging from 0.5 to 300 μm . When utilized as an admixture, fly ash, following the primary cement hydration process to produce $\text{Ca}(\text{OH})_2$, undergoes the secondary hydration reactions, known as pozzolanic reactions. This results in the formation of calcium silicate hydrate (C-S-H) gel, which fills the internal micropores of soils, refines the pore sizes, and consequently enhances the mechanical properties of soil structures (Kolias et al., 2004; Mousavi, 2018; Ni et al., 2021). Presently, fly ash remains an underutilized industrial byproduct, with a lack of widespread implementation of reasonable recovery and

resource utilization practices (Guo, 2009; Jongpradist et al., 2010; Wang et al., 2019). The power industry's rapid development has led to an annual increase in fly ash emissions. Statistics reveal that burning 3–4 tons of raw coal generates 1 ton of fly ash (Xu et al., 2021; Gao, 2023). In the years of 2010, 2015, and 2021, China's fly ash emissions were 300 million tons, 620 million tons, and 790 million tons, respectively (Jiang, 2020; Xu et al., 2021). Given the significant annual production of fly ash, improper disposal into the atmosphere can result in air pollution. Moreover, the accumulation of substantial amounts of fly ash can generate airborne dust, causing severe contamination in the surrounding environment, presenting health hazards, and placing additional burdens on businesses. This, in turn, reflects an inefficient utilization of valuable resources.

Currently, significant emphasis has been placed on investigating the resource utilization of fly ash. Cui et al. (2012), through experimental studies, determined that a high dosage of fly ash can substantially enhance the later strength of cemented soil, identifying the optimal fly ash-to-cement ratio as 3.0. Cristelo et al. (2012) investigated the impact of calcium content in fly ash on the strength of solidified soil. Their results suggested that, under alkaline activation, the early strength of high-calcium fly ash solidified soil can rapidly increase. Focusing on saturated loess in the Lanzhou region, Yang et al. (2016) replaced a portion of cement with fly ash in cemented soil. They found that, with a constant amount of binder material, the unconfined compressive strength of fly ash-cemented soil slightly decreased with an increase in fly ash content. Meng et al. (2017), conducted a study on the strength of cemented soil from the Shanghai Suzhou River area with fly ash through unconfined compressive strength tests. Their results indicated that, with an increase in fly ash content and curing age, the behavior of cemented soil gradually changed from plastic failure to brittle failure. Duan and Zhang (2019) explored the influence of fly ash and polypropylene fibers on the unconfined compressive strength of cemented soil, and demonstrated that when the content of fly ash and polypropylene fiber was 8.0% and 0.4%, respectively, the unconfined compressive strength reached its peak. Cui et al. (2019) studied the impact of sodium silicate and fly ash on the permeability of cemented soil. They found that, with a constant sodium silicate content, the addition of fly ash reduced the permeability coefficient of cemented soil. It was also noted that the permeability coefficient of fly ash-cemented soil decreased with an increase in curing age. Zhang et al. (2020), using Guangzhou Nansha soft clay as raw material, conducted model tests to study the strength of fly ash-cemented soil. The results revealed a trend of increasing the strength with a higher fly ash content, reaching a peak at 15% fly ash content. Luis and Deng (2020), studied the strength of fly ash-cemented soil and observed its internal structure using scanning electron microscopy. The results showed that the addition of fly ash can disperse cement, reduce cement clusters, and thereby improve the later strength of cemented soil. Yang et al. (2021) investigated the influence of fly ash on the mechanical properties of arsenic sandstone-cemented soil. They found that the strength growth rate of arsenic sandstone-cemented soil slowed down when the fly ash content exceeded 12%. Ding et al. (2021) adopted the technique of scanning electron microscopy to examine the impact of fly ash on the mechanical properties of cemented soil. The results indicated that the addition of fly ash can reduce the internal pores of cemented soil, enhancing the structural density. Zhang et al. (2024) utilized a

sequential extraction procedure (SEP) and potential risk assessment index to evaluate the long-term stability risk of fly ash-based cementitious materials containing arsenic (FCAC). Fly ash, serving as a substitute for cement, has garnered the interest of researchers in the realm of pile foundation engineering. Phanikumar et al. (2009) highlighted the potential of fly ash columns (FAC) in mitigating swell–shrink problems associated with expansive soils. Their study revealed significant reductions in heave and improved stress–settlement characteristics with FAC reinforcement. Zheng et al. (2011) discussed ground improvement using cement-fly ash-gravel piles in the construction of the Beijing-Tianjin high-speed railway over soft marine clay. Field measurements revealed reduced excess pore pressure and settlement, with pile compression making a minimal contribution. Zhang et al. (2017) investigated the use of steel-slag concrete with fly ash as a composite foundation pile material for ground improvement. They demonstrated that this approach can achieve high bearing capacity, minimal settlement, and limited horizontal deformation, showcasing the potential of fly ash in pile composite foundations.

Stiffened deep cement mixing (SDCM) piles represent an innovative form of composite pile foundation. The construction process involves vertically embedding concrete core pile into cement mixing pile prior to the initial set of cement-soil mixture. This composite pile capitalizes on the advantages of substantial lateral frictional resistance present in cement mixing pile socket, coupled with the high strength exhibited by concrete core pile. Wu and Zhao, (2006) conducted model tests on SDCM piles, and identified that under equivalent pile diameters and lengths, the vertical bearing capacity of SDCM piles was 2.7–3.6 times greater than that of cement mixing piles. Li et al. (2009) emphasized that stress concentration could most likely occur in the core pile section of SDCM piles. Field experiments conducted by Jamsawang et al. (2010) observed that the increase in length ratio between core pile and cement mixing pile, as well as the cross-sectional area ratio between these two components, substantially improved the vertical bearing capacity of SDCM piles. Liu et al. (2010) used a large-scale geotechnical testing model trench to conduct static load tests for both SDCM piles and bored cast-in-place piles. They discovered that, under the same pile length and diameter, the vertical bearing capacity of SDCM piles was more than 30% higher than that of bored cast-in-place piles. Voottipruex et al. (2011) and Bergado et al. (2011) revealed that, when compared to cement mixing piles, SDCM piles exhibited a notable reduction in uneven settlement deformation in roadbeds. Voottipruex et al. (2011) performed model tests and numerical simulations to understand the vertical bearing mechanism of SDCM piles. Their findings suggested that the friction coefficient between concrete core pile and cement mixing pile ranged from 0.35 to 0.43. Huang, (2013) found that appropriately increasing the cement content can enhance the strength of SDCM piles to some extent. However, in practice, exceeding a cement content of 20% is not advisable due to the cost consideration and the easiness in construction. Zhang et al. (2013) observed that the load transfer in SDCM piles could follow a two-layer mode, where the pile top load was firstly transmitted from the core pile to the cement mixing pile and then from the cement mixing pile to the surrounding soil. Srijaoren et al. (2021) introduced soil-cement screw piles (SCSP) as an innovative piling solution in soft Bangkok clay. They advocated for the economic and operational advantages of SCSP, potentially

influencing construction practices. Zhou et al. (2022) carried out field experiments and numerical simulations, from which they discovered that the vertical bearing capability of SDCM piles increased proportionally with the increase of cement content until the pile underwent punching failure. Amjad et al. (2022) introduced an extreme gradient boosting (XGBoost) model for predicting the load-bearing capacity of pile foundations. Their sensitivity analysis underscored the importance of Standard Penetration Test (SPT) blow count. Hoy et al. (2023) compared soil-cement columns (SC), stiffened soil-cement columns (SSC), and sheet pile walls as retaining structures in shallow excavations within soft Bangkok clay through finite element simulations. Their study highlighted the superior efficiency of SC walls in terms of both time and cost. Practical demonstrations have revealed a notable enhancement in the bearing capacity of DCM piles through the integration of core piles (Bergado et al., 2009; Liu et al., 2010). The impact of core pile penetration on DCM piles encompasses primarily two facets: 1) the compaction of the DCM pile is notably intensified, leading to an augmentation in the density of cement-treated soils; 2) the DCM pile undergoes radial expansion, resulting in an increase in pile diameter.

Despite the extensive investigations carried out by researchers on the SDCM pile-soil interaction mechanisms, there is currently limited study on the application of fly ash as a high-performance admixture in SDCM piles. The mechanical properties of pile materials improved by fly ash are not yet clear. This study extends the existing literature on fly ash-treated Stiffened Deep Cement Mixing (SDCM) piles by focusing specifically on the vertical bearing mechanism through laboratory model tests. Firstly, it compares the performance of fly ash-treated SDCM piles with that of standard SDCM piles, facilitating a direct assessment of the impact of fly ash substitution on the vertical bearing capacity and settlement characteristics of the piles. Such a comparative analysis enhances the practical relevance of the study's findings and provides valuable insights for engineers and practitioners. Secondly, by investigating the hydration rates of fly ash relative to cement and analyzing the settlements at different curing durations, the study offers insights into the time-dependent behavior of fly ash-treated SDCM piles. This adds a temporal dimension to the understanding of

pile performance, which may not have been thoroughly explored in previous literature. Lastly, the study utilizes fly ash from a specific source (Class F category of low-calcium fly ash originating from a power plant in Taiyuan). This specificity underscores the potential variability in fly ash properties and its implications for the performance of SDCM piles. It also emphasizes the importance of considering the characteristics of fly ash used in practical applications. The objectives of the study are as follows:

- Investigation of the correlation between pile top load and pile top settlement, taking into account various fly ash contents and curing ages;
- Analysis of the axial force of core pile, the interfacial frictional force between core pile and cement mixing pile, and the pile end resistance for fly ash-treated SDCM piles.

Experimental program

Materials

A clayey soil from Taiyuan, China, with the properties outlined in Table 1, was used as the foundation soil. According to the Unified Soil Classification System, this soil was categorized as low plasticity clay (CL). The clayey soil was backfilled and compacted within the model box, utilizing a vibratory plate compactor.

This study comprised four sets of model tests, designated as Case 1 to Case 4. DCM piles, each with a diameter of 100 mm and a length of 1.0 m, were constructed using ordinary Portland cement (OPC 42.5). The amounts of cementitious materials (e.g., cement and fly ash), alkali activator (e.g., calcium hydroxide), curing duration, and water/binder ratio are detailed in Table 2. The fly ash originated from a power plant located in Taiyuan. It belongs to the Class F category of low-calcium fly ash, with its chemical composition detailed in Table 3. It is noted that the amounts of cementitious materials and alkali activator were characterized by the dry mass ratio to the soil. To replicate the behavior of core pile, a solid PVC plastic rod measuring 50 mm in diameter and 600 mm in length was utilized.

TABLE 1 Physical properties of soil.

Water content (%)	Density (g/cm ³)	Liquid limit (%)	Plastic limit (%)	Optimum water content (%)	Maximum dry density (g/cm ³)
14.1	1.8	26.5	16.1	15	1.85

TABLE 2 Summary of model tests.

Case	Cement content (%)	Fly ash content (%)	Calcium hydroxide (%)	Curing duration (d)	Water/binder ratio
1	20	0	0	7	1
2	14	6	1	7	1
3	20	0	0	28	1
4	14	6	1	28	1

TABLE 3 Chemical composition of fly ash.

	SiO ₂	Al ₂ O ₃	Fe ₂ O ₃	CaO	MgO	SO ₃
Content (%)	51.43	34.05	5.02	3.31	0.564	1.61

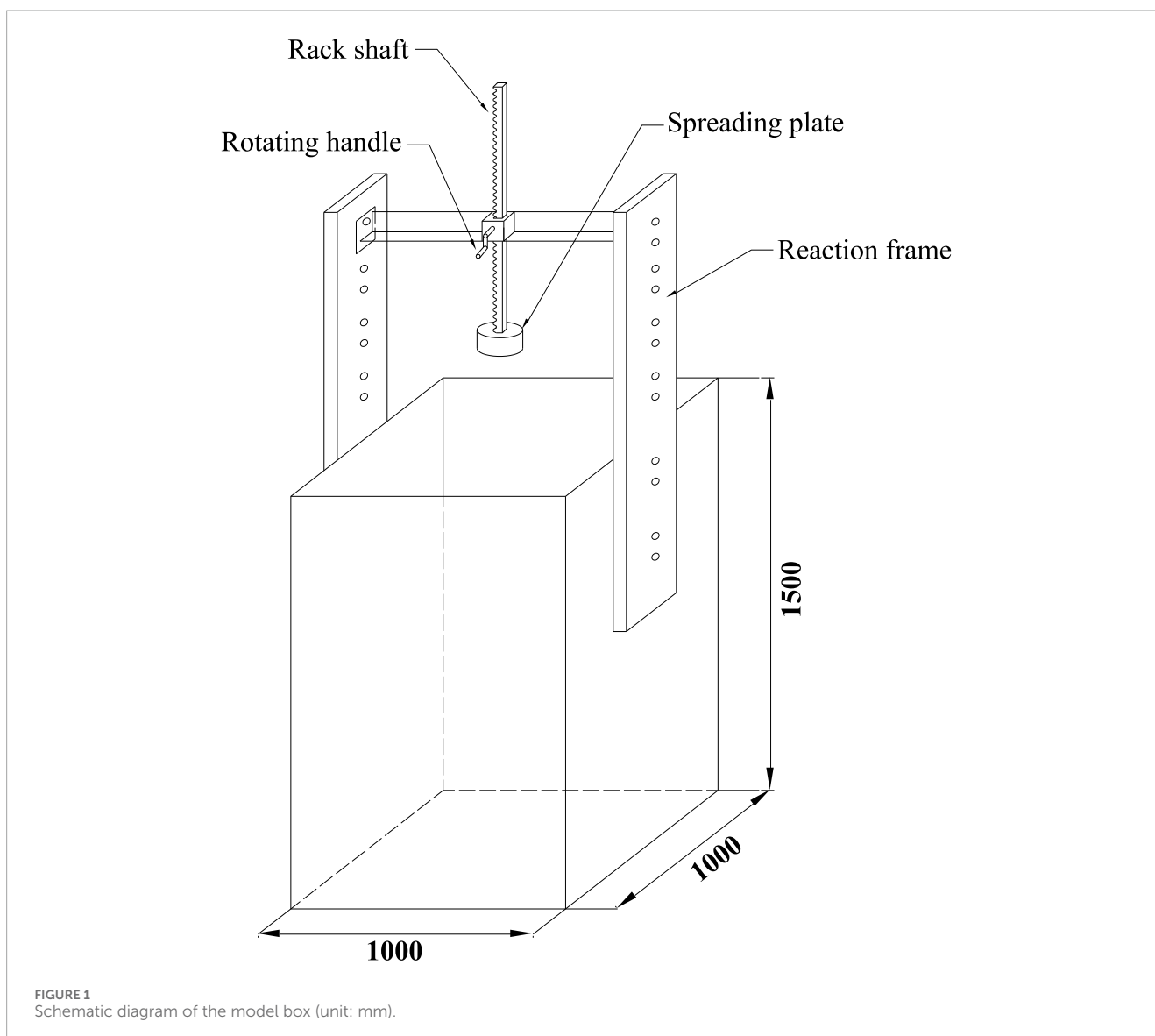
Test apparatus

The physical model box, depicted in Figure 1, was constructed with 20-mm-thick steel plates and measured 1.0 m in length, 1.0 m in width, and 1.5 m in height. To minimize the boundary effect, the distance from the SDCM pile to the container's sidewall was established at 4.5 times the pile diameter (i.e., 450 mm/100 mm) (Zhou et al., 2022). The model box were equipped with a reaction frame through bolted connections. A gear-rack drive device, fixed on the reaction frame, facilitated the insertion of core pile into DCM pile before the initial setting of cement-stabilized soils. Core pile

was held through a spreading plate on a rack shaft and gradually advanced into DCM pile by rotating the handle. Rotating the handle twice resulted in a downward movement of core pile by 10 mm.

Instrumentation

The vertical load on the pile top was applied using a hydraulic jack (FCY-10150) manufactured by Taizhou Jugong Hydraulic Equipment Ltd., featuring a maximum stroke of 150 mm. To measure the pile top load, a GY-2 load cell from ACCU-Champ Inc., featuring a measuring range of 98 kN and an accuracy of 0.02% full scale (FS), was employed. To gauge the tip resistance, an earth pressure cell (MAS-SPG-02) produced by MAS Ltd., equipped with a measuring range of 2.0 MPa, was positioned beneath the pile end. For measuring the settlement of pile top, a string potentiometer (MPS-S-2000-R-F) manufactured by Shenzhen Milont Technology Ltd. was employed, which featured a range of 2000 mm and an accuracy of 0.15% full scale (FS). Optical fibers were attached along



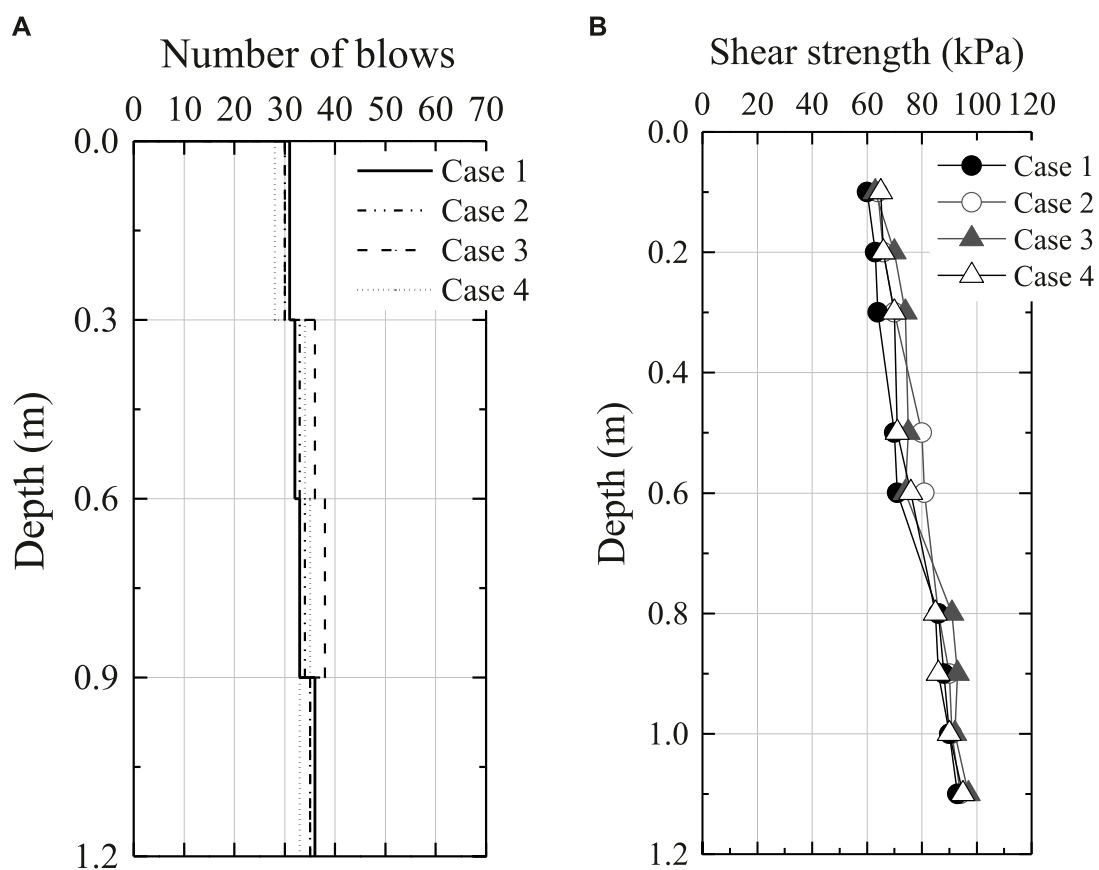


FIGURE 2 Results of compacted soil strength in Cases 1 to 4: (A) DCPTs; (B) vane shear test.

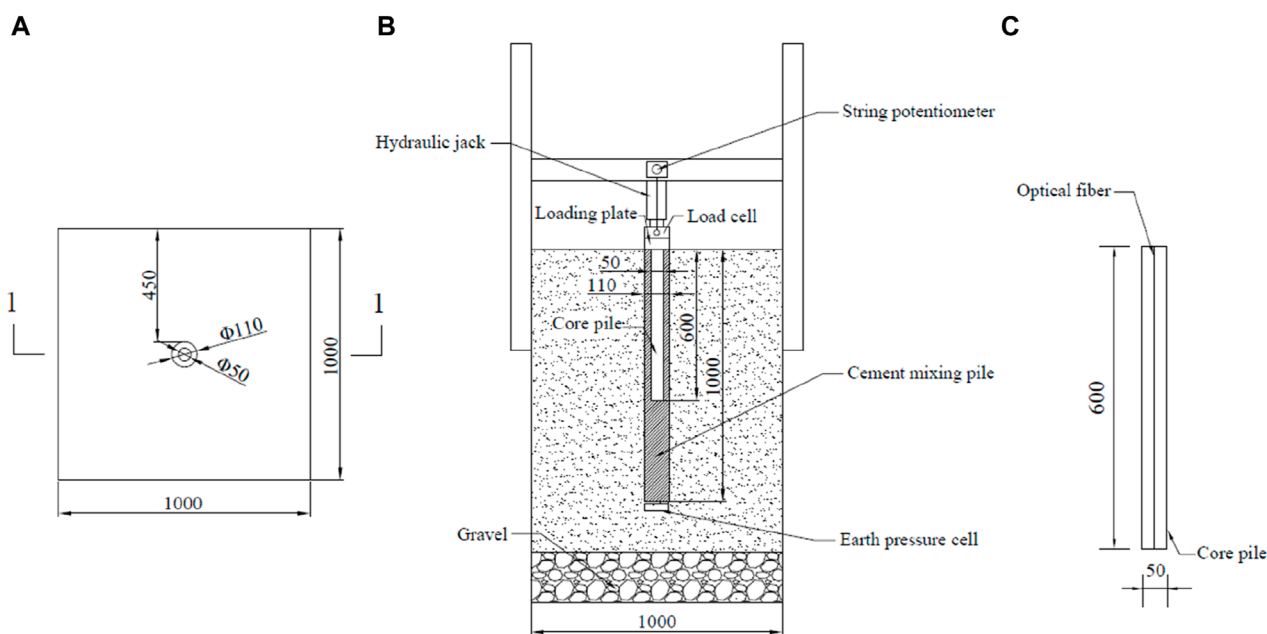
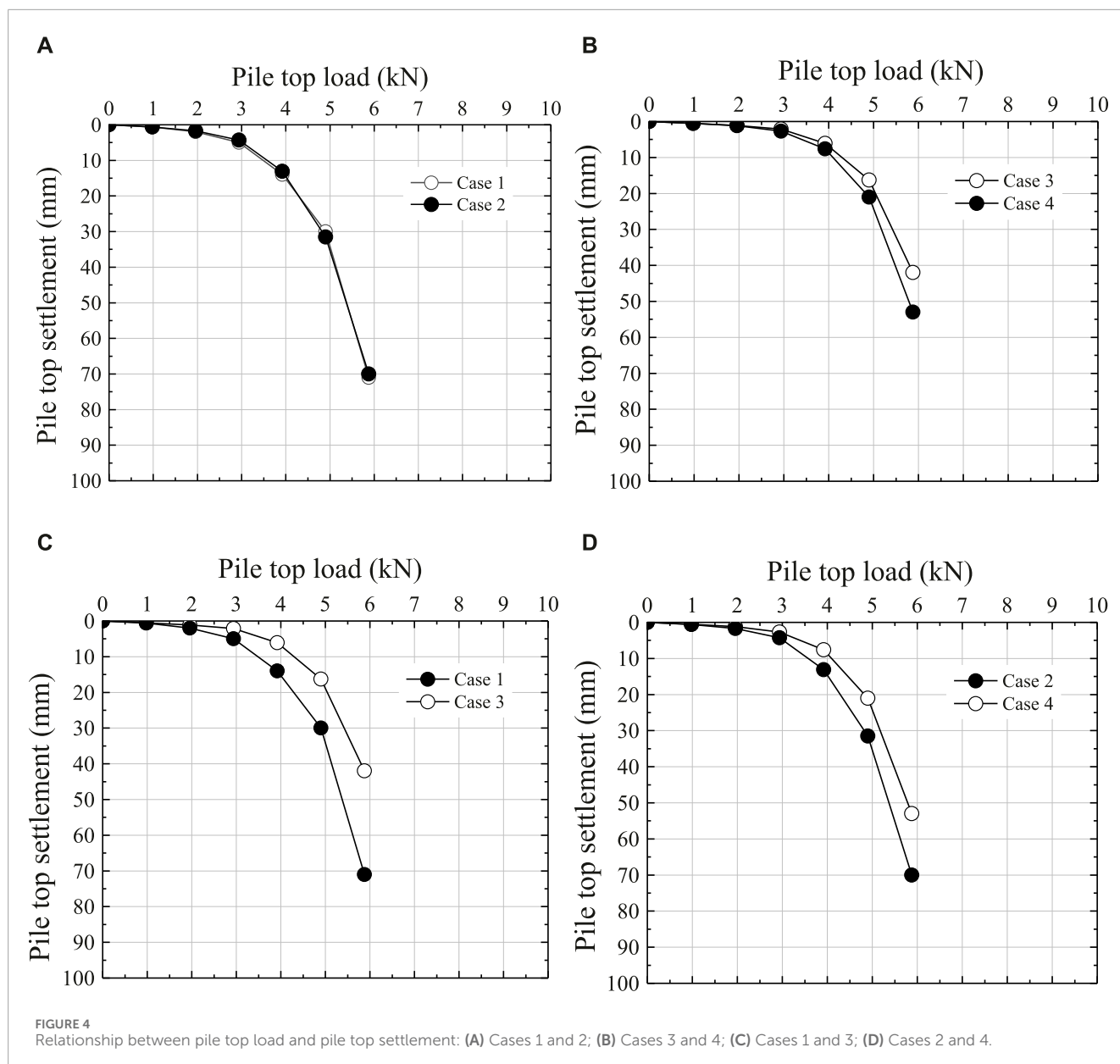


FIGURE 3 Loading diagram of SDCM pile: (A) plan view; (B) Section 1-1; (C) optical fiber arrangement (unit: mm).



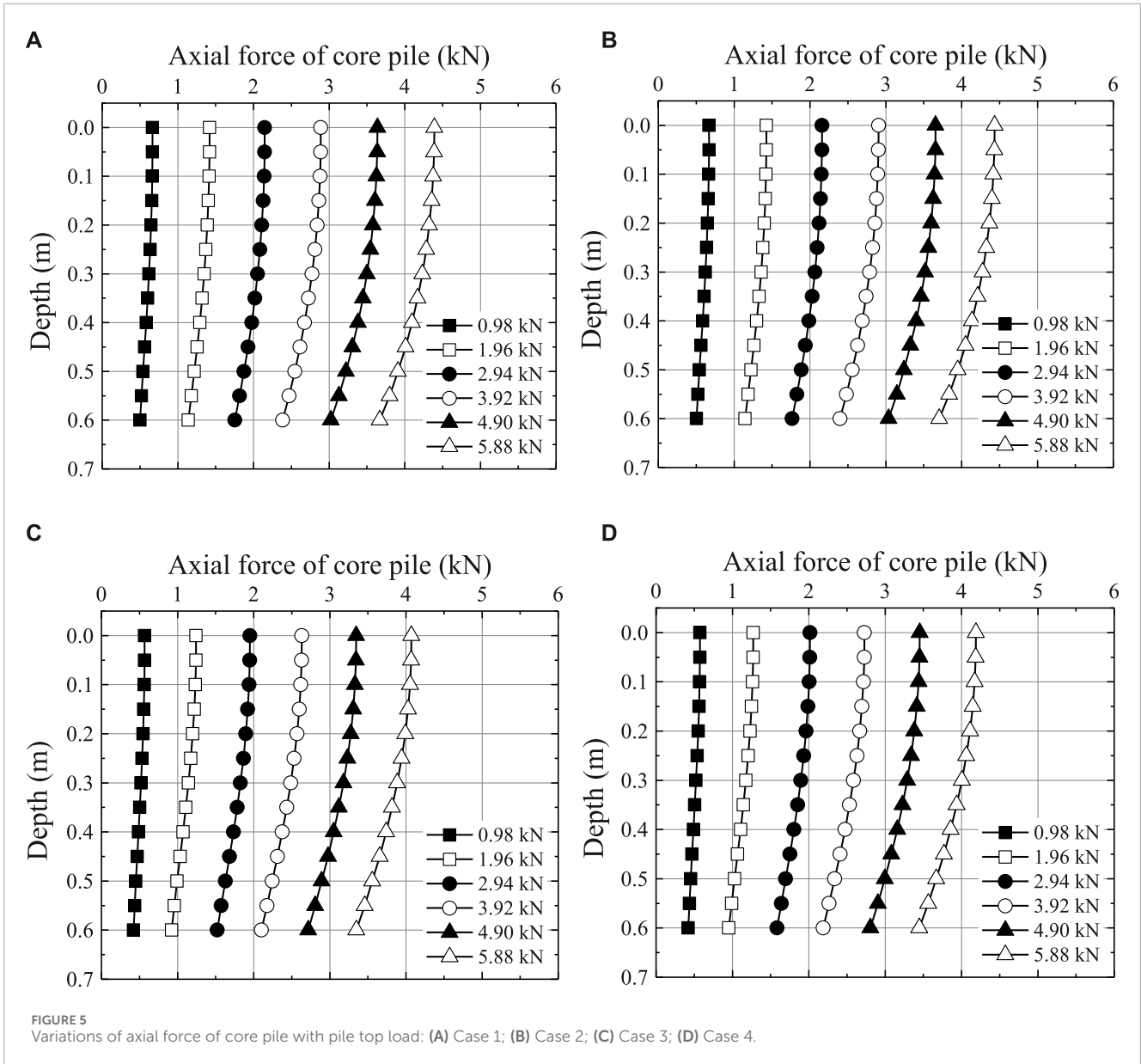
the axis of core pile to monitor the distributed pile strains. They could boast a measurement range of 20,000 microstrain ($\mu\epsilon$) and an accuracy of $10 \mu\epsilon$.

Test method

Following the completion of test setup, the bearing capacity and shear strength of foundation soil were assessed through dynamic cone penetration test (DCPT) and vane shear test, respectively, in accordance with ASTM D6951/D6951M (ASTM, 2009) and ASTM D4648/D4648M (ASTM, 2013). It is worth noting that the backfilling and compaction of clayey soils were carried out utilizing a vibratory plate compactor. Each case study was tested only once in this investigation. However, in terms of the repeatability of the model tests, unconfined compressive strength tests were conducted

on cement-treated soil specimens prior to testing. Three parallel specimens were tested for each mix proportion to effectively control the variability of the physical properties of cement-treated soil. To reduce the variability in the soil surrounding the piles, compaction tests and DCPT were conducted before backfilling to measure the relationship between compaction effort and soil resistance as determined by DCPT. Figure 2A illustrates the count of blows for advancing the cone penetrometer through the soil at increments of 0.3 m penetration depth. Figure 2B presents the changes in vane shear strength of soil with depth. It is evident that in all cases, the bearing capacities and vane shear strength of surrounding soils at various depths were nearly identical.

The construction of SDCM pile proceeded through the following steps: 1) a 0.2 m thick gravel layer with a compaction degree of 90% was initially backfilled in the model box. Subsequently, the clayey soil was backfilled and compacted to establish a 0.2 m thick bedding

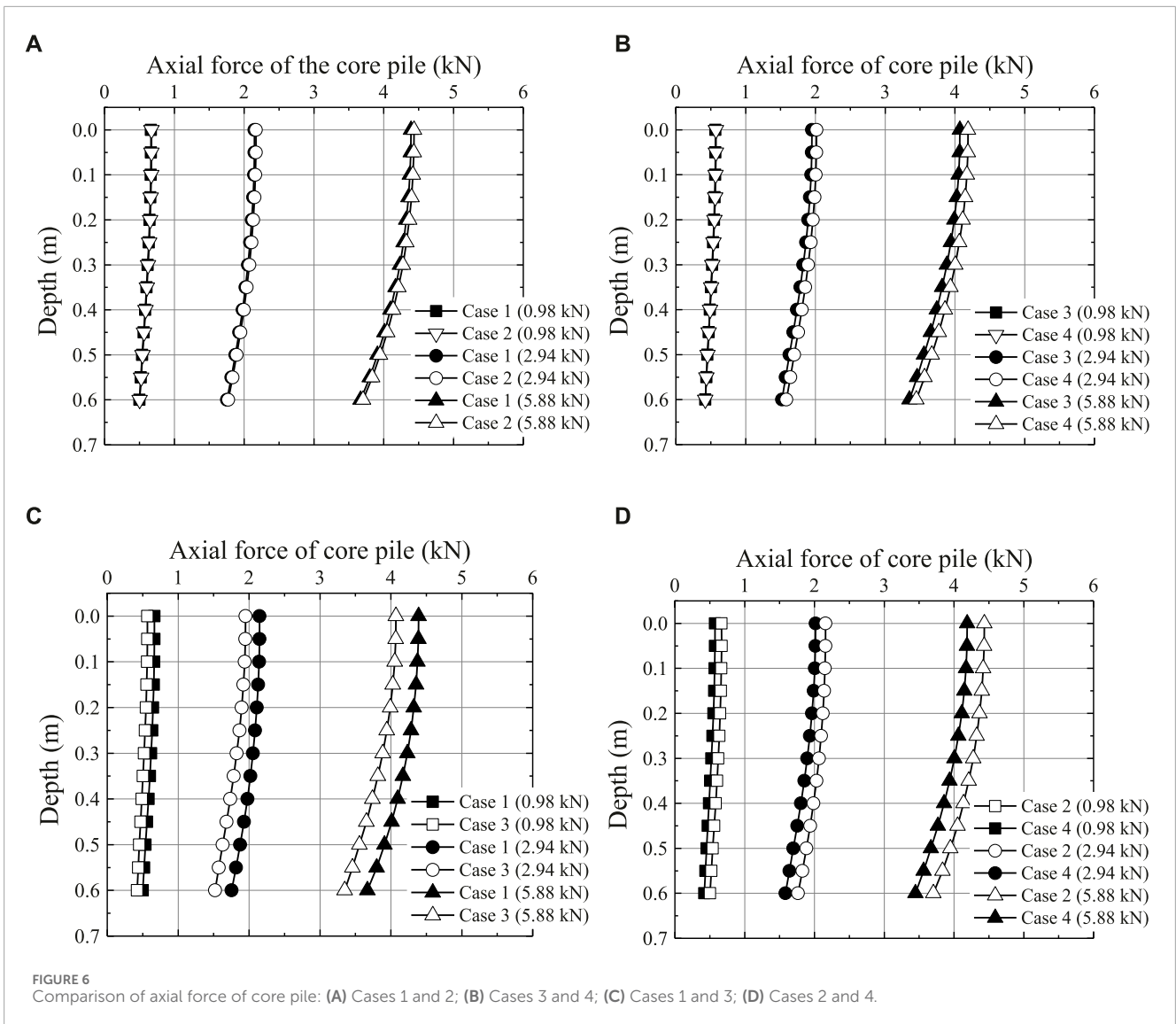


layer; 2) a PVC tube with a diameter of 100 mm and a length of 1.0 m was positioned at the center of the model box. To mitigate the boundary effects, the distance from the tube edge to the sidewall of the model box was set at 4.0 times the tube diameter; 3) the soil was placed around the PVC tube and compacted in layers, each with a thickness of 0.3 m per lift, until reaching the intended soil surface; 4) a uniformly stirred soil-cement slurry was poured into the PVC tube to create the cement mixing pile. Vibration was applied using a handheld vibrator during this process; 5) the PVC tube was removed, and subsequently, a 50 mm-diameter solid PVC plastic rod, measuring 600 mm in length, was concentrically inserted into the soil-cement slurry before its initial setting.

The rationale behind selecting a thickness of 0.2 m for both the gravel layer and the clayey soil layer in Step 1) encompasses several factors, including considerations related to structural stability, drainage efficiency, and compaction requirements. Firstly, a 0.2 m thick gravel layer serves as a stable foundation, distributing loads

evenly and minimizing settling. Similarly, a 0.2 m thick bedding layer of clayey soil provides a stable base for subsequent construction layers. Secondly, with a 0.2 m thick gravel layer, there is ample space for water to seep through, reducing the risk of water-related issues such as suffusion or soil saturation. Moreover, the clayey soil layer above the gravel can act as a filter barrier, further enhancing drainage capabilities. Lastly, maintaining a uniform thickness, such as 0.2 m, streamlines the compaction process, allowing for consistent efforts to achieve the desired density throughout the layers. This uniformity plays a pivotal role in ensuring the stability and performance of the overall structure.

Figure 3 depicts the loading diagram of SDCM pile in the model test, as well as the configuration of optical fiber attached along the core pile. Vertical loading on the pile top was implemented in stages, precisely at 0.98 kN, 1.96 kN, 2.94 kN, 3.92 kN, 4.9 kN, and 5.88 kN, adhering to the guidelines outlined in JGJ 106-2014. Specifically, loading increments were set at 1/12 to 1/10 of the estimated ultimate



bearing capacity of the pile. Each loading level was maintained for approximately 5 min, and the test was terminated when the rate of pile settlement exceeded 1.0 mm/s.

Test results

Figure 4 shows the relationship between pile top load and pile top settlement (i.e., load-settlement curve) in Cases 1 to 4. It is seen from Figure 4A that the settlements at the pile top measured in Case 1 are almost the same with those measured in Case 2, indicating that under alkaline activation, the early hydration rate of fly ash closely resembles that of cement. Figure 4B shows that the pile top settlements measured in Case 4 are greater than those measured in Case 3. It illustrates that as the curing age increases, the hydration rate of fly ash gradually becomes lower than that of cement. As expected, the settlements measured at the pile top, cured for 28 days in Cases 3 and 4, are significantly smaller than those cured for 7 days in Cases 1 and 2, as shown in Figure 4C and 4d).

The axial force of core pile can be calculated using the measured distributed strains by optical fiber through Eq. 1:

$$N = EA\varepsilon \tag{1}$$

where N is the axial force of core pile (kN); E is the elastic modulus of core pile (kPa); A is the cross-sectional area of core pile (m^2); and ε is the axial strain of core pile, which can be measured using an optical fiber. It notes that the elastic modulus of core pile, a solid PVC plastic rod used in the model tests, was determined to be 3,000 MPa, as specified by the manufacturer.

Figure 5 presents the variations of axial force of core pile in Cases 1 to 4 with pile top load. It is observed that the axial force of core pile is raised with an increase in pile top load, while it decreases with depth. More specifically, the axial forces at the core pile end in Cases 1 to 4 represent 75%–83%, 70%–81%, 74%–82%, and 73%–82%, respectively, of those at the top of core pile. This suggests the activation of frictional forces along the interface between core pile and cement mixing pile socket.

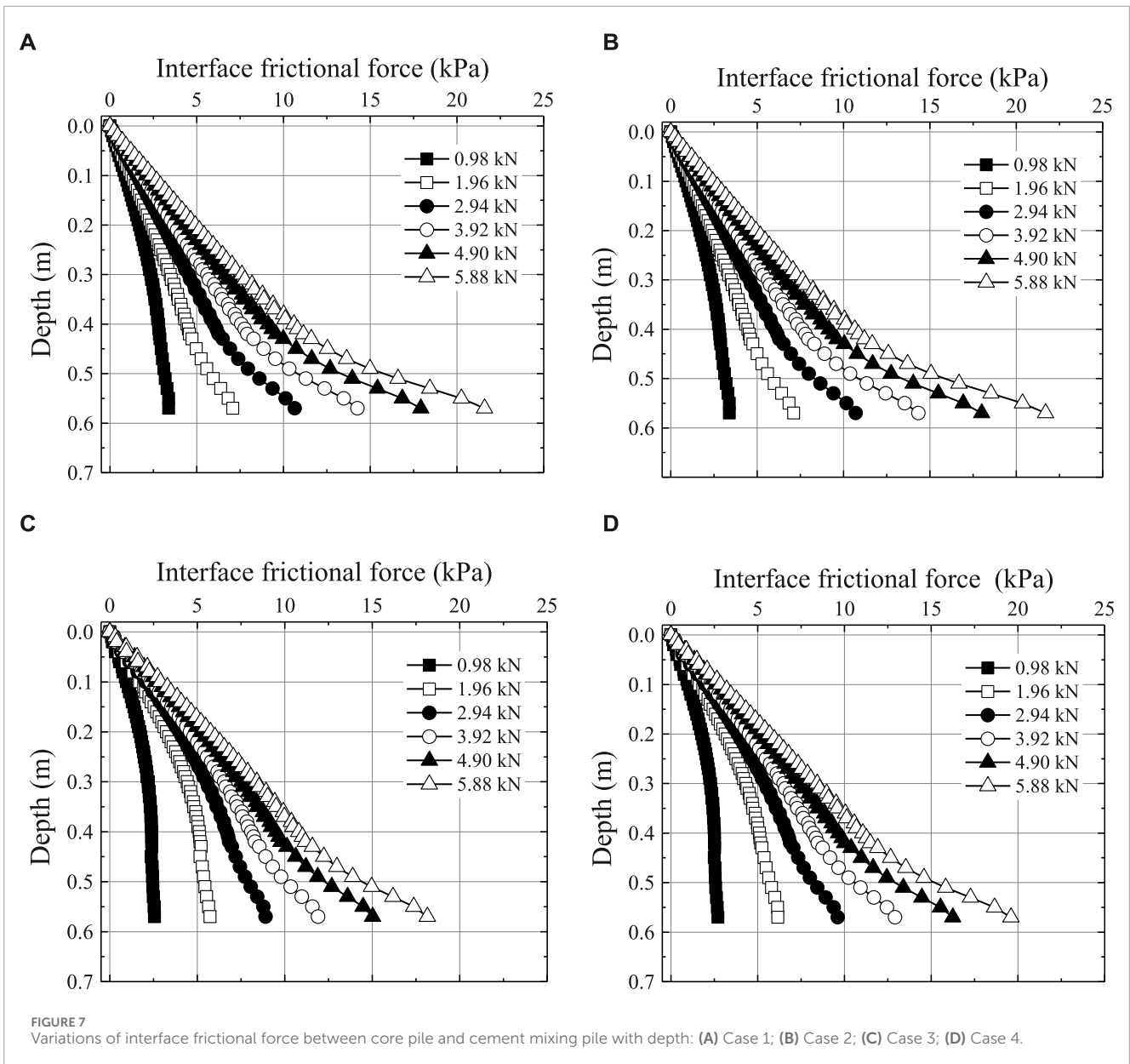


FIGURE 7 Variations of interface frictional force between core pile and cement mixing pile with depth: (A) Case 1; (B) Case 2; (C) Case 3; (D) Case 4.

Figure 6 illustrates the comparison of axial force of core pile under only three levels of pile top loads of 0.98 kN, 2.94 kN, and 5.88 kN, enhancing clarity for comparison purposes. In Figure 6A, the discrepancy between axial forces of core piles in Cases 1 and 2 is minimal. This can be attributed to the shorter curing time (i.e., 7 days), leading to lower hydration levels in the soil mixing piles for both Cases 1 and 2. Consequently, the disparities in hydration rates between fly ash and cement are less pronounced, resulting in minimal differences in the axial forces of core piles between Cases 1 and 2. Moving to Figure 6B, it is evident that the axial forces of core pile in Case 4 surpass those in Case 3. Examining Figure 6C and 6d, the axial forces of core piles, cured for 7 days in Cases 1 and 2, exceed those cured for 28 days in Cases 3 and 4. This suggests that when the hydration level of cement mixing pile socket is low, leading to a decreased stiffness, the core pile bears a greater vertical load.

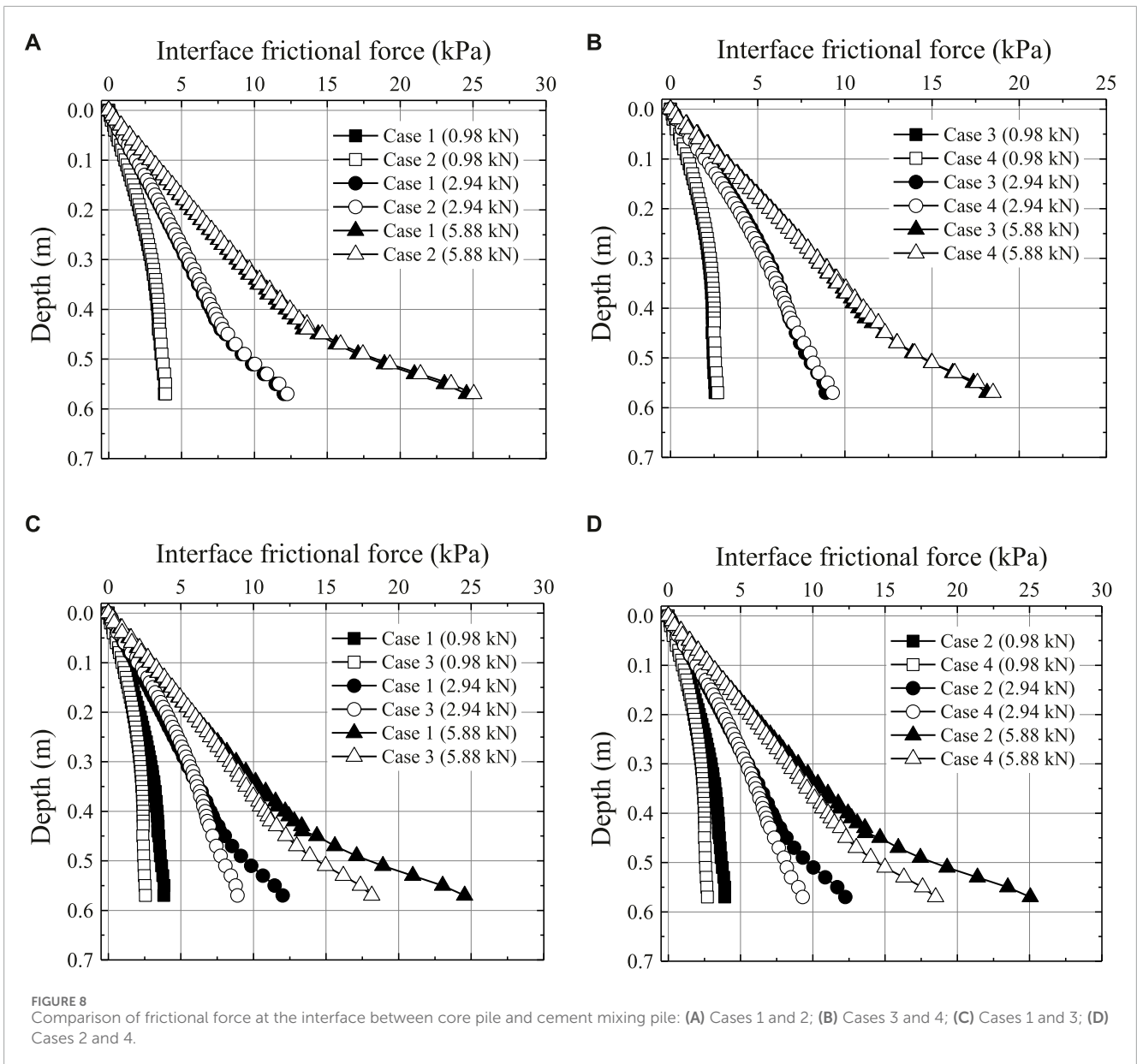
The interface frictional force between core pile and cement mixing pile socket can be obtained by Eq. 2, which is derived

based on the principle of static equilibrium (Zhou et al., 2022; Zhu et al., 2022):

$$f = \frac{\Delta N}{\pi D \Delta h} \tag{2}$$

where f is the interface frictional force (kPa); ΔN and Δh are the difference in axial force (kN) and distance (m), respectively, between two adjacent strain data points measured by optical fiber; and D is the diameter of core pile (m).

Figure 7 shows the variations of frictional force at the interface between core pile and cement mixing pile socket in Cases 1 to 4 as a function of depth. It is seen that the interface frictional force increases gradually with depth. Figure 8 compares the interface frictional forces between core pile and cement mixing pile socket under the pile top loads of 0.98 kN, 2.94 kN, and 5.88 kN. It is seen from Figure 8A and 8b) that the difference in interface frictional force is minimal between Cases 1 and 2, and a similar situation is

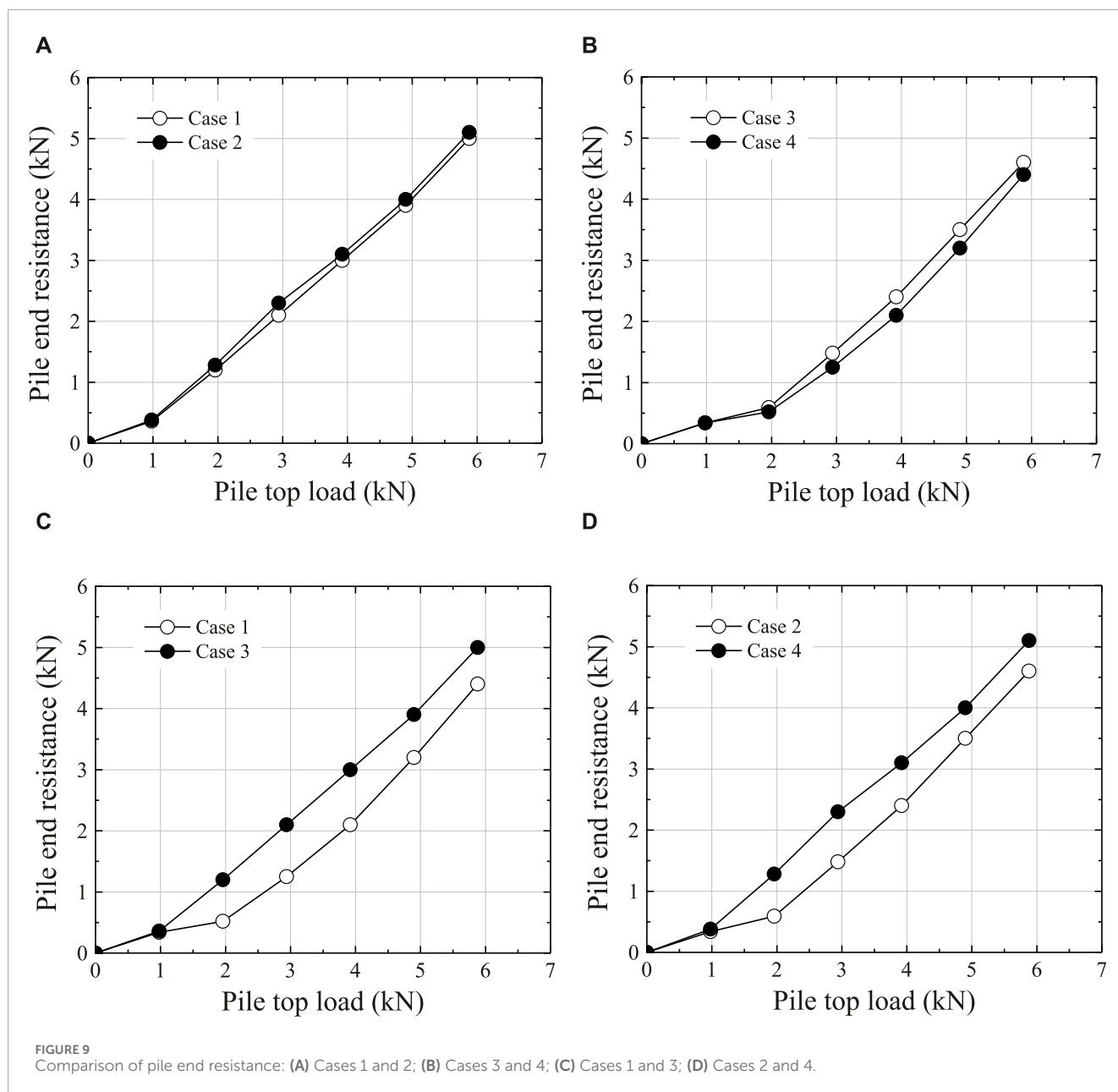


observed for Cases 3 and 4. Additionally, Figure 8C and 8d) indicate that the interface frictional force decreases with the increase of curing period.

Figure 9 shows the comparison of pile end resistance under varying pile top loads. Figure 9A indicates a minimal variation in pile end resistance between Cases 1 and 2. In Figure 9B, the pile end resistances in Case 3 surpass those in Case 4. Figure 9C and 9d) further demonstrate that the pile end resistances in Cases 3 and 4 exceed those in Cases 1 and 2, respectively. This suggests that the pile end resistance increases when the hydration level of soil mixing pile socket is higher, leading to an elevated stiffness. This is because that the hydration reactions occurring between cement, fly ash, and water in soil mixing piles can result in the creation of cementitious compounds, such as calcium silicate hydrate (C-S-H) gel, within the soil, associated with volume changes. This process can result in compaction and densification in the surrounding soil, significantly enhancing the pile's end resistance and stiffness.

Discussions

Utilizing Buckingham's Pi-theorem, the model test was devised incorporating eight similitude criteria, i.e., $\pi_1 = FL_d^{-2}E_d^{-1}$, $\pi_2 = \gamma L_d E_d^{-1}$, $\pi_3 = E_s E_d^{-1}$, $\pi_4 = D_c L_d^{-1}$, $\pi_5 = L_c L_d^{-1}$, $\pi_6 = E_c E_d^{-1}$, $\pi_7 = D_d L_d^{-1}$, $\pi_8 = c E_d^{-1}$. These criteria encompass various parameters such as the load applied at the pile top (F), the length, diameter and elastic modulus of the DCM pile (L_d , D_d and E_d), the unit weight and cohesion of the soil (γ and c), the soil modulus (E_s), the length, diameter and elastic modulus of the core pile (L_c , D_c and E_c). Scaling down the size of the model pile by a factor of 1:10 compared to the prototype allowed for effective simulation of real-world conditions. According to the second similitude criterion (π_2), the unit weight of the soil required scaling up by a factor of 10 while keeping the elastic modulus of the DCM pile unchanged. All model tests were conducted under 1-g conditions, indicating a limitation of the study as the stress field in the soil could



not be accurately replicated. Nevertheless, the study focuses on a DCM pile with specific dimensions (110 mm diameter and 1.0 m length) constructed using ordinary Portland cement (OPC 32.5). The core pile behavior was simulated with a solid PVC plastic rod (50 mm diameter and 600 mm length). These choices were informed by engineering experience, considering the typical ranges of DCM and core pile dimensions found in literature (Yi et al., 2016; Liu et al., 2020). By scaling down and conducting model tests, valuable insights into the features of pile-soil interaction crucial for SDCM pile construction in real-world scenarios can be gained.

The addition of fly ash to cementitious systems, such as SDCM piles, initiates pozzolanic reactions and induces microstructural changes that significantly impact the pile performance. These pozzolanic reactions contribute to the densification and

strengthening of the cementitious matrix, leading to increased strength and stiffness of SDCM pile. This improvement in mechanical properties enhances the load-bearing capacity and overall performance of the pile. Furthermore, the incorporation of fly ash alters the microstructure of the cementitious matrix by generating additional hydration products like C-S-H gel and calcium aluminate hydrates. These added hydration products fill the pore spaces within the matrix, resulting in a denser and more compact structure. Consequently, this densification enhances various mechanical properties of the pile, including compressive strength, stiffness, and durability.

For projects prioritizing rapid construction or facing significant time constraints, a shorter curing duration of 7 days is viable. This timeframe is suitable when immediate load-bearing capacity is needed, although it may result in slightly lower stiffness and

pile end resistance compared to the case with a longer curing duration. It is suitable for projects where an acceptable difference in settlement between the top of a fly ash-treated SDCM pile and a standard SDCM pile exists. Conversely, for projects emphasizing maximizing stiffness and pile end resistance, opting for a longer curing duration of 28 days is recommended. This extended period allows for more complete hydration of both cement and fly ash, leading to heightened stiffness and enhanced pile end resistance. This is particularly crucial in situations prioritizing the structural integrity and long-term performance, such as high-rise buildings or critical infrastructure projects. When balancing construction time and pile performance is necessary, a compromise between the two curing durations could be appropriate. For instance, a duration between 7 and 28 days, such as 14 or 21 days, could strike a reasonable balance between achieving adequate strength and stiffness while minimizing construction time. This approach is suitable for projects where moderate settlement at the top of the pile is acceptable, but optimizing pile performance is still a priority. Ultimately, selecting the optimal curing duration should involve a thorough consideration of project-specific requirements, including construction timelines, budget constraints, and performance expectations. Collaborating with engineers, contractors, and stakeholders to assess these factors will facilitate informed decision-making regarding the most suitable curing duration for a given project.

SDCM piles are a type of ground improvement technique used in geotechnical engineering to strengthen weak soils. While SDCM piles offer several advantages, such as increased bearing capacity, reduced settlement, and improved stability, they also face specific limitations and challenges in research and application. Firstly, the long-term behavior of SDCM piles remains incompletely understood, complicating predictions regarding their performance over extended durations. Secondly, the development of design guidelines for SDCM piles is ongoing, and standardized construction techniques are lacking. Construction parameters such as cement content and inserting rate of core pile into the DCM pile often rely on empirical data. Lastly, the environmental impact of SDCM, encompassing concerns about groundwater contamination and carbon footprint of cementitious materials, requires attention. Recommendations to address these issues include the establishment of long-term monitoring programs to gather information on pile deformation, cement-stabilized soil properties, and environmental factors, thus facilitating the study of SDCM pile performance over time. Additionally, fostering knowledge exchange among researchers, engineers, and construction professionals is essential for creating comprehensive design guidelines and construction standards for SDCM piles. Lastly, exploring the adoption of eco-friendly cementitious materials and recycling techniques can mitigate the environmental footprint associated with SDCM piles.

Conclusion

Four series of laboratory model tests were carried out to examine the vertical bearing capacity of SDCM piles. This was necessary because, following the application of loading on the pile top, the piles subjected to a curing duration of 7 days incurred damage and

were unable to undergo further curing for 28 days. Additionally, this investigation advances the current understanding of using fly ash in SDCM piles for ground improvement by providing insights into its environmental, economic, and mechanical implications. By exploring the use of fly ash as a partial substitute for cement in SDCM piles, the study addresses environmental concerns associated with the disposal of fly ash, which is an industrial byproduct. Through testing SDCM piles with different fly ash contents (0% and 6%), the study contributes to optimizing the mix design of these piles, offering insights into the effects of fly ash on their mechanical properties and performance. This aids engineers and practitioners in making informed decisions regarding material selection. The examination of curing periods (7 and 28 days) furnishes valuable information on the time-dependent behavior of fly ash-treated SDCM piles. Understanding how curing duration influences the hydration rates of fly ash and its impact on pile settlement and stiffness facilitates improved planning and optimization of construction schedules. Through laboratory model tests, the study elucidated the vertical bearing mechanism of fly ash-treated SDCM piles, analyzing how variations in fly ash content and curing period affect the settlement behavior, stiffness, and pile end resistance, thereby contributing to a deeper understanding of the performance of these piles under different conditions. The key findings from this investigation are outlined below:

- (1) Settlements at the top of SDCM piles in Cases 1 and 2 are nearly identical, indicating comparable early hydration rates of fly ash under alkaline activation as compared to cement. However, with increase of curing age, the hydration rates of fly ash become lower than those of cement, as evidenced by greater pile top settlements in Case 4 compared to Case 3.
- (2) The axial force of core pile is calculated using distributed optical fiber strains, showing an increasing pattern with a higher pile top load and a decreasing trend with depth. Core pile's axial forces represent a significant contribution at the top, suggesting that the frictional forces along the interface between core pile and cement mixing pile socket are mobilized.
- (3) Frictional force at the interface between core pile and cement mixing pile increases gradually with depth. Interface frictional force differences are minimal between Cases 1 and 2, as well as between Cases 3 and 4. Additionally, interface frictional force decreases with an increase in curing period.
- (4) Pile end resistance variation is observed between different conditions, with Case 3 showing a higher resistance than Case 4, and Cases 3 and 4 exhibiting greater resistance than Cases 1 and 2. The results suggest that higher hydration levels in soil mixing pile can lead to an increased pile end resistance and stiffness.

Data availability statement

The raw data supporting the conclusion of this article will be made available by the authors, without undue reservation.

Author contributions

MZ: Conceptualization, Data curation, Investigation, Methodology, Writing—original draft, Writing—review and editing. WZ: Conceptualization, Data curation, Methodology, Writing—review and editing. YH: Conceptualization, Data curation, Writing—review and editing. Changyi Tang: Data curation, Writing—review and editing.

Funding

The author(s) declare that financial support was received for the research, authorship, and/or publication of this article. The experiment was funded by the Applied Basic Research Program of Shanxi Province of China (202303021221110).

References

- Amjad, M., Aslam, A., Shoaib, M., Ahmed, A., Kamiński, P., and Amjad, U. (2022). Prediction of pile bearing capacity using XGBoost algorithm: modeling and performance evaluation. *Appl. Sci.* 12 (4), 2126. doi:10.3390/app12042126
- ASTM (2009). "Standard test method for use of the dynamic cone penetrometer in shallow pavement applications," in *ASTM D6951/D6951M-09. Annual book of ASTM standards* (West Conshohocken, PA: ASTM).
- ASTM (2013). "Standard test method for laboratory miniature vane shear test for saturated fine-grained clayey soil," in *Annual book of ASTM standards. ASTM D4648/d4648m-13* (West Conshohocken, PA: ASTM).
- Bergado, D. T., Phienweij, N., Jamsawang, P., Ramana, G. V., Lin, S. S., and Abuel-Naga, H. M. (2009). "Settlement characteristics of full scale test embankment on soft Bangkok clay improved with Thermo-PVD and stiffened deep cement mixing piles," in *Proceedings of the 17th International Conference on Soil Mechanics and Geotechnical Engineering* (Alexandria, Egypt: IOS Press), 1969–1972.
- Bergado, D. T., Voottipruex, P., and Jamsawang, P. (2011). Field behaviour of stiffened deep cement mixing piles. *Proc. Institution Civ. Eng. Ground Improv.* 164 (1), 33–49. doi:10.1016/j.grim.900027
- Cristelo, N., Glendinning, S., Fernandes, L., and Pinto, A. T. (2012). Effect of calcium content on soil stabilisation with alkaline activation. *Constr. Build. Mater.* 29, 167–174. doi:10.1016/j.conbuildmat.2011.10.049
- Cui, J. Y., Xie, B. L., Ji, G. A., Ji, X., and Zhang, W. Y. (2019). Experimental study on the permeability of fly ash soil-cement. *Sci. Technol. Eng.* 19 (34), 323–329.
- Cui, Y. C., Cui, Z. Z., Zhou, J., Zhou, K., and Zhang, M. (2012). Research on mechanical properties of fly ash cement soil in Yinchuan. *Ind. Constr.* 42 (7), 105–109+151. doi:10.13204/j.gyjz2012.07.002
- Ding, X. Q., Guo, Y. Z., Zhao, L. J., and Fang, Y. F. (2021). Effects of fly ash on the mechanical properties of soil-cement. *Non-Metallic Mines* 44 (2), 50–52+56.
- Duan, X. L., and Zhang, J. S. (2019). Mechanical properties, failure mode, and microstructure of soil-cement modified with fly ash and polypropylene fiber. *Adv. Mater. Sci. Eng.* 2019, 1–13. doi:10.1155/2019/9561794
- Gao, Z. Q. (2023). *Experimental study on air barrier performance of fly ash as flame retardant covering layer of coal gangue hill*. Shanxi: North University of China. Master thesis.
- Guo, X. L. (2009). *Research on comprehensive utilization technology of fly ash in coal-fired power plants*. Xi'an, Chang'an University: Master thesis.
- Hoy, M., Srijaroen, C., Horpibulsuk, S., Phunpeng, V., Rachan, R., and Arulrajah, A. (2023). Innovative solution: soil cement column walls as a temporary retaining structure for excavation in soft Bangkok clay. *Smart Constr. Sustain. Cities* 1 (1), 19. doi:10.1007/s44268-023-00017-z
- Huang, X. L. (2013). *The model test and analysis of the modified stiffening core soil-cement composite pile in Yellow River flooded area*. Master thesis. Kaifeng: Henan University.
- Jamsawang, P., Bergado, D. T., and Voottipruex, P. (2010). Field behaviour of stiffened deep cement mixing piles. *Proc. ICE-Ground Improv.* 164 (1), 33–49. doi:10.1680/grim.900027
- Jiang, L. (2020). Comprehensive utilization situation of fly ash in coal-fired power plants and its development suggestions. *Clean. Coal Technol.* 26 (4), 31–39. doi:10.13226/j.issn.1006-6772.F19062501
- Jongpradist, P., Jumlongrach, N., Youwai, S., and Chucheeprakul, S. (2010). Influence of fly ash on unconfined compressive strength of cement-admixed clay at high water content. *J. Mater. Civ. Eng.* 22 (1), 49–58. doi:10.1061/(asce)0899-1561(2010)22:1(49)
- Kolias, S., Kasselouri-Rigopoulou, V., and Karahalios, A. (2004). Stabilisation of clayey soils with high calcium fly ash and cement. *Cem. Concr. Compos.* 27 (2), 301–313. doi:10.1016/j.cemconcomp.2004.02.019
- Li, J. C., Deng, Y. G., Song, G. H., and Ling, G. H. (2009). Analysis of load-bearing mechanism of composite foundation of plain concrete reinforced cement-soil mixing piles. *Rock Soil Mech.* 30 (1), 181–185. doi:10.16285/j.rsm.2009.01.041
- Liu, H. L., Ren, L. W., Zheng, H., and Xiao, Y. Z. (2010). Full-scale model test on load transfer mechanism for jet grouting soil-cement-pile strengthened pile. *Rock Soil Mech.* 31 (5), 1395–1401. doi:10.16285/j.rsm.2010.05.041
- Liu, S. Y., Zhou, J., Zhang, D. W., Ding, X. M., and Lei, H. Y. (2020). State of the art of the ground improvement technology in China. *China Civ. Eng. J.* 53 (4), 93–110. doi:10.15951/j.tmgxcb.2020.04.009
- Luis, A., and Deng, L. J. (2020). Development of mechanical properties of Edmonton stiff clay treated with cement and fly ash. *Int. J. Geotechnical Eng.* 14 (3), 329–339. doi:10.1080/19386362.2018.1454387
- Meng, Q., Shao, L., and Shi, Q. Y. (2017). Experimental study on the mechanical properties of fly ash cement soil. *J. Univ. Shanghai Sci. Technol.* 39 (5), 490–496. doi:10.13255/j.cnki.jusst.2017.05.013
- Ministry of Housing and Urban Rural Development of the People's Republic of China (2014). *Technical code for testing of building foundation piles*. Beijing: China Architecture and Building Press, 106–2014. JGJ.
- Mousavi, S. E. (2018). Utilization of silica fume to maximize the filler and pozzolanic effects of stabilized soil with cement. *Geotechnical Geol. Eng.* 36 (1), 77–87. doi:10.1007/s10706-017-0305-x
- Ni, J., He, Q. Q., Li, S. S., Ma, L., and Zhang, S. L. (2021). Correlation between macroscopic mechanical strength and microstructure of fly ash cement soil under combined effect of water pollution and freeze-thaw cycles. *J. Changjiang River Sci. Res. Inst.* 38 (9), 97–104.
- Phanikumar, B. R., Mani, A. J., Sathiyasheelan, S., and Rajesh Reddy, P. (2009). Fly ash columns (FAC) as an innovative foundation technique for expansive clay beds. *Int. J. 4* (3), 183–188. doi:10.1080/17486020902857007
- Srijaroen, C., Hoy, M., Horpibulsuk, S., Rachan, R., and Arulrajah, A. (2021). Soil-cement screw pile: alternative pile for low- and medium-rise buildings in soft Bangkok clay. *J. Constr. Eng. Manag.* 147 (2), 04020173. doi:10.1061/(asce)co.1943-7862.0001988
- Voottipruex, P., Bergado, D. T., Suksawat, T., Jamsawang, P., and Cheang, W. (2011). Behavior and simulation of deep cement mixing (DCM) and stiffened deep cement mixing (SDCM) piles under full scale loading. *Soils Found.* 51 (2), 307–320. doi:10.3208/sandf.51.307
- Voottipruex, P., Suksawat, T., Bergado, D. T., and Jamsawang, P. (2011). Numerical simulations and parametric study of SDCM and DCM piles under full scale axial and lateral loads. *Comput. Geotech.* 38, 318–329. doi:10.1061/41165(397)85

Conflict of interest

Author MZ was employed by Shanxi Construction Investment Group Co., Ltd.

The remaining authors declare that the research was conducted in the absence of any commercial or financial relationships that could be construed as a potential conflict of interest.

Publisher's note

All claims expressed in this article are solely those of the authors and do not necessarily represent those of their affiliated organizations, or those of the publisher, the editors and the reviewers. Any product that may be evaluated in this article, or claim that may be made by its manufacturer, is not guaranteed or endorsed by the publisher.

- Wang, Y., Huang, Y. Y., Fang, G. B., Huang, X. Q., Cai, R., and Yin, X. F. (2019). Experimental study on the performance of fly ash cement soil in the Dongting Lake area. *J. Water Resour. Water Eng.* 30 (4), 210–216.
- Wu, M., and Zhao, X. (2006). Bearing behaviors of stiffened deep cement mixed pile. *Trans. Tianjin Univ.* 12 (3), 209–214.
- Xu, S., Yang, J., and Ma, S. (2021). Research progress in the comprehensive utilization of fly ash. *Conservation Util. Mineral Resour.* 41 (3), 104–111. doi:10.13779/j.cnki.issn1001-0076.2021.03.015
- Yang, J., Li, X. L., Wang, H., and Geng, K. Q. (2021). Indoor experimental study on mechanical properties of composite fly ash and Pisha-sandstone cement soil. *J. Drainage Irrigation Mach. Eng.* 39 (12), 1230–1236.
- Yang, Y. H., Liu, Y. H., and Ren, X. (2016). Experimental research on the factors influencing strength of cement-mixed saturated loess. *J. Railw. Eng. Soc.* 33 (1), 21–25+64.
- Yi, Y., Liu, S., and Puppala, A. J. (2016). Laboratory modelling of T-shaped soil-cement column for soft ground treatment under embankment. *Géotechnique* 66 (1), 85–89. doi:10.1680/jgeot.15.p.019
- Zhang, B., Cui, S., Liu, Z., and Feng, F. (2017). Field tests of cement fly-ash steel-slag pile composite foundation. *J. Test. Eval.* 45 (3), 860–872. doi:10.1520/jte20140422
- Zhang, M., Wu, Y., Li, Y., Zhou, R., Yu, H., Zhu, X., et al. (2024). Risk assessment for the long-term stability of fly ash-based cementitious material containing arsenic: dynamic and semidynamic leaching. *Environ. Pollut.* 345, 123361. doi:10.1016/j.envpol.2024.123361
- Zhang, P. F., Wu, W., and Liu, Z. J. (2020). Experimental analysis of the influence of fly ash on the strength of cement soil. *Build. Tech. Dev.* 47 (9), 144–146.
- Zhang, Y. G., Li, J. C., and Deng, Y. G. (2013). Experimental study of load transfer mechanism of composite pile of jet-mixing cement and PHC pile. *J. Nanjing Univ. Technol. Nat. Sci. Ed.* 35 (06), 79–85.
- Zheng, G., Jiang, Y., Han, J., and Liu, Y. F. (2011). Performance of cement-fly ash-gravel pile-supported high-speed railway embankments over soft marine clay. *Mar. Georesources Geotechnol.* 29 (2), 145–161. doi:10.1080/1064119x.2010.532700
- Zhou, M., Li, Z. T., Han, Y. S., Ni, P. P., and Wang, Y. L. (2022). Experimental study on the vertical bearing capacity of stiffened deep cement mixing piles. *Int. J. Geomechanics* 22 (5), 04022043. doi:10.1061/(asce)gm.1943-5622.0002355
- Zhu, S., Chen, C., Cai, H., and Mao, F. (2022). Analytical modeling for the load-transfer behavior of stiffened deep cement mixing (SDCM) pile with rigid cap in layer soils. *Comput. Geotechnics* 144, 104618. doi:10.1016/j.compgeo.2021.104618